

Evidence for metastable excimer states as the source of electron train backgrounds in liquid xenon emission detectors

P. Sorensen^{1,*} and K. Kamdin^{1,2}

¹*Lawrence Berkeley National Laboratory, 1 Cyclotron Rd., Berkeley, CA 94720, USA*

²*University of California Berkeley, Department of Physics, Berkeley, CA 94720, USA*

(Dated: December 2, 2023)

Single electron backgrounds with millisecond timescales are known to follow ionizing events in liquid/gas xenon emission detectors. These backgrounds can limit the low-energy threshold of dark matter searches, and prevent discovery-class searches for MeV scale hidden sector dark matter. A systematic study reveals a fast (τ_1) and slow (τ_2) component to the background. The fast component is compatible with electrons which were trapped at the liquid surface, and can be reduced by increasing the electric field. However, the slow component increases linearly with electric field. This is consistent with electron impact excitation of higher-energy molecular excited states. Several techniques for mitigation are suggested.

I. INTRODUCTION

Liquid xenon emission detectors [1] are a variant of the time projection chamber in which ionized electrons are drifted to the liquid-gas interface under the influence of an applied electric field E_l . There, they are extracted, drifted through the gas and amplified via proportional scintillation. This technique can easily provide sensitivity to single electrons. It has been known for decades that the bulk of the electron emission from the liquid into the gas proceeds in a time $t \lesssim 1$ ns, and that there also exists a field-dependent component of the emission with $\tau \gtrsim 0.1$ ms [2]. A widely accepted interpretation is that this is due to thermalization of electrons at the interface. Recently, the XENON10 Collaboration identified a single electron background, referred to as an “electron train,” with a time scale at least as long as the putative thermalized component [3].

There is great interest in mitigating this background. It is a potential irritation in the analysis of dark matter search data from instruments such as LUX [4] or XENON1T [5], where it can complicate the classification of low-energy events. And it greatly diminishes the discovery potential of these detectors for MeV-scale hidden sector dark matter [6], in which the expected signal from scattering events is a single ionized electron [7]. Recognizing this, the proposed $U_{A'}$ (1) experiment [8] aspires to deploy a 10-kg scale liquid xenon emission detector, free from electron train backgrounds.

In this article we report results of R&D towards that end, from a systematic study of electron trains in a small liquid xenon emission detector. The data clearly show two components τ_1 and τ_2 in the electron train, the faster of which τ_1 can reasonably be interpreted as the initially un-emitted (thermalized) electrons. However, the slower component τ_2 is not at all consistent with this hypothesis. Instead, as will be argued, it is more likely due to an

afterglow emission of photons which then photo-ionize impurities in the liquid xenon.

II. EXPERIMENTAL DETAILS

The test bed used to obtain these results was configured with a 50 mm diameter wire grid cathode and planar, segmented anode. The stainless steel wires had 100 μ m diameter and were spaced on a 2 mm pitch. The anode and the cathode were located 5 mm apart, and ~ 650 g of liquid xenon were introduced, until the liquid level was about 4 mm above the cathode. An electric field E_l was applied in the z direction by biasing the cathode to a voltage $-V$, and holding the anode at ground. Electrons resulting from ionizing radiation were thus drifted toward the anode, and extracted across the liquid-gas interface. The value of E_l contains a systematic uncertainty of ± 0.4 kV/cm due to uncertainty in the liquid xenon level. This relationship is described in the Appendix. This uncertainty does not affect the basic results, but should be born in mind when comparing against other measurements. Aqueous ^{210}Po (as PoCl_4) was evaporated on a single section of a single wire, in the center of the cathode. The literature does not discuss spontaneous deposition of polonium onto stainless steel [9], however, we found it to be robust against dissolution in liquid xenon. The source spot size was such that alpha particle signals only appeared on the charge preamplifier connected to the central, 6 mm diameter anode pad. This arrangement was made in order to mitigate the effects of electric field fringing near the edges of the active region.

A single Hamamatsu R8778 VUV-sensitive photomultiplier was installed 10 mm below the cathode grid. The photomultiplier was biased to the recommended maximum -1500 V, resulting in easily recognizable single photoelectron pulses and a gain of 1.9×10^7 . Voltage records of ionizing radiation events were digitized at 14 bits with 125 MHz sampling and a 20 MHz low-pass filter, with an event duration of 1 ms. Typical events contained both a primary scintillation pulse (S1) and a secondary,

* pfsorensen@lbl.gov

proportional scintillation pulse (S2) caused by extracted electrons. The S2 signal was verified to be extremely linear, with the number of detected photons increasing as $y = 10 \cdot (V - 1.9)$. A helium after-pulse (a photomultiplier artifact) was often evident 500 ns after the S1. The 5.3 MeV alpha particles result in an average 380,000 quanta (electrons and photons) in the liquid xenon, of which an electric-field-dependent 91.3% (lowest E_l data point) to 81.6% (highest E_l data point) appeared as 7.1 eV primary scintillation photons, with the remainder as ionized electrons. These signals were sufficient to saturate the biasing circuit of the photomultiplier, precluding an accurate measurement of the number of electrons present in the alpha S2. Despite this, (a) the alpha particle population was easily identifiable by its size and characteristic drift time (from the cathode), and (b) the number of electrons obtained from alpha particle pulses was measured separately with the charge-sensitive preamplifier.

During operation, the xenon was maintained at a vapor pressure of 1.5 Bar, with a cryostat temperature of 174 K. It was continuously circulated through a heated getter. The liquid was evaporated into the purification loop via a capillary, and the gas was separately purged into the purification loop via a sintered metal filter (to limit the purge rate). The xenon turnover time was about 6 hours, as measured by mass flow. About 2/3 of the flow rate was from the liquid, and the rest from the gas purge. The electron attenuation length was not measured during this experiment, but from comparison with previous experiments and measured charge yields in the literature, can be inferred to have improved to a few tens of cm over a week.

III. RESULTS AND DISCUSSION

Data were acquired at four values of E_l , corresponding to $V = [3, 4, 5, 6]$ kV. In each case, the population of ^{210}Po alpha particle events was isolated using simple, robust software cuts on the signal size of S1, S2 and the time delay between them. The waveforms were summed and the decay time of the electron train was obtained by fitting a linear function to $y = \log[\Sigma(\alpha \text{ events})]$ over 40 μs (τ_1) and 500 μs (τ_2) regions, indicated by the extent of the fits in Fig. 1 (bottom). The τ_1 fit region was chosen to begin 40 μs after the S2, to ensure fidelity of the photomultiplier signal. The number of single electrons in these regions were counted. Separately, the number of electrons was measured with the charge sensitive preamplifier.

The fast (τ_1) and slow (τ_2) components were assumed to begin immediately after the primary event, and extend to infinity. The measured amplitudes a_1 and a_2 of each component were corrected for the sample window, and are plotted in Fig. 2 as a percent of the measured number of electrons. Two data sets are plotted for each value of E_l : data points offset to the left of each E_l were acquired shortly after condensing xenon into the test bed, and

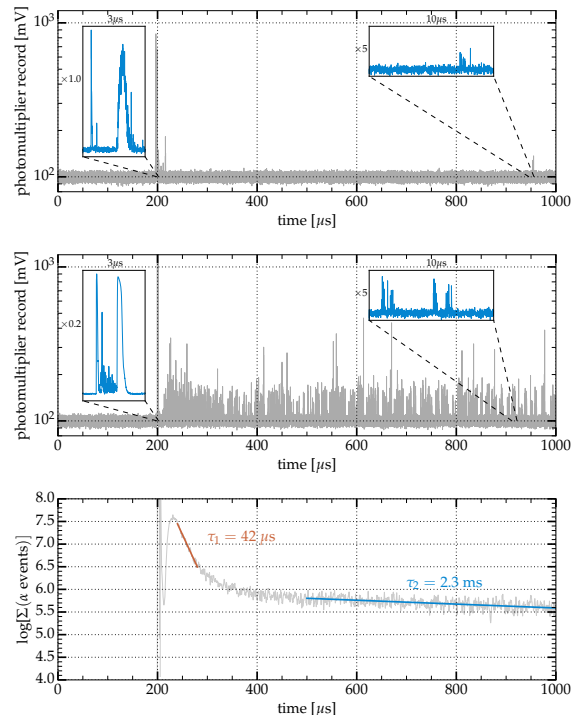


FIG. 1. Typical ^{206}Pb and ^{210}Po alpha particle events with $V = 4$ kV, showing inset detail of the primary S1 and S2 structure of the event, as well as a zoom on a portion of the after-pulse region. **(top)** A ^{206}Pb recoil event record, with S1=130 detected photons and S2=67 electrons. A single electron is visible nearly 800 μs after the primary event. **(middle)** A ^{210}Po alpha particle event record. **(bottom)** 400 summed alpha particle event records, low-pass filtered to more clearly illustrate the electron train.

data points offset to the right of each E_l were acquired a week later.

The amplitude a_1 decreases with increasing E_l , suggesting that these are the thermalized, un-emitted primary electrons. This interpretation can be compared against $(1 - \kappa)$, where κ is the electron emission efficiency (expressed as a percent). The parameterizations $\kappa = [1 + \exp(\frac{5}{3}(-E_l + 3))]^{-1}$ and $\kappa = [1 + \exp(1.14 \cdot (-E_l + 3.41))]^{-1}$ were fit to the data from [2, 10]. Assuming the measurements of [10] to be correct, it would appear that for $E_l < 7$ kV/cm about half of the thermalized electrons are never emitted. This is consistent with capture by electronegative impurities before they can escape into the gas.

On the other hand, the amplitude a_2 increases linearly with increasing E_l , suggesting an origin due to the number proportional scintillation photons. A distinct reduction in the size of the slow component of the electron train is obtained by purifying the xenon. This suggests that at times $t \gtrsim 5\tau_1$, the single electrons in the electron train are due to photoionization of impurities.

It has been known for at least half a century [11] that liquid xenon scintillates in the vacuum ultraviolet, due to

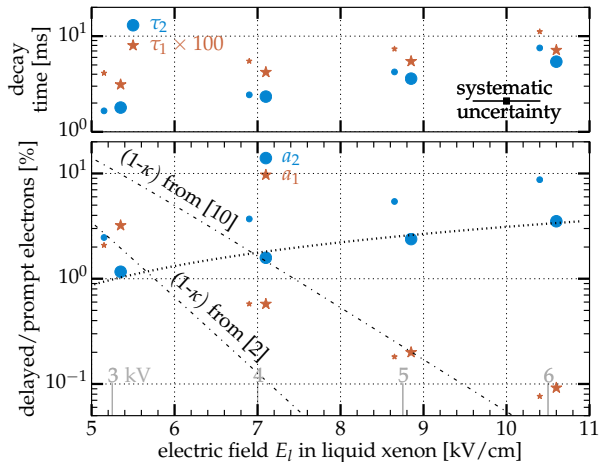


FIG. 2. For each cathode potential (indicated along the x axis), two data points are shown. The smaller points (offset to the left) were obtained while liquid xenon purity was relatively poor compared with the larger points (offset to the right). Systematic uncertainty in E_l applies to all points. Statistical uncertainty is comparable to the size of the points. **(top)** The measured decay times τ_1 and τ_2 . The error bars on each E_l are instrumental only, and apply to data points in the lower panel as well. **(bottom)** The amplitude of the electron train as a percent of the original number of electrons in the ionizing event, as a function of E_l . The fast component τ_1 can be compared against $(1 - \kappa)$, where κ is the electron emission efficiency. The slow component τ_2 is fit by a linear function (dotted).

formation of excimers with ~ 1 eV binding energy. Later work categorized (e.g.) the decay times of the singlet $^1\Sigma_u^+$ and triplet $^3\Sigma_u^+$ states [12], which are a few to a few tens of nanoseconds. Data are sparse concerning bound states in heavy noble gas excimers, but additional higher-energy states are expected to be weakly bound [13].

Detailed calculations of the Xe_2^* potential curves [14] show two sets of higher-energy bound states, transition from one of which appears to be electric-dipole forbidden. It is natural to expect that the process of proportional scintillation (electron impact excitation) in xenon populates not only $^1,3\Sigma_u^+$ states, but higher states as well. If transition from the latter to the former were governed by a lifetime greater than a few milliseconds, it could explain (i) the observed decay time of the electron train (ii) its linear increase with E_l and (iii) the significant increase in number of isolated single photoelectrons we observe amongst the single electrons in electron trains.

We do not have a physical explanation for the increase in τ_1 with E_l . It may be an artifact of the fit, since a_1 is decreasing in amplitude while a_2 increases. If the excited molecular state interpretation of a_2 is correct, then the increase of τ_2 with E_l could be due to the electric field reducing the overlap of the excited electron's wave function with those of the core electrons.

Care must be taken with the interpretation of the measured decay constants τ_1 and τ_2 . In the limit of a static

xenon fluid with perfect purity, τ_1 would be the thermalized electron emission time and τ_2 would be the lifetime of the metastable state. In actuality, the value of τ_1 is likely shortened by the capture time of electrons by electronegative impurities. The value of τ_2 is likely shortened by the physical flow of gas atoms out of the region where their emitted photons can be detected.

IV. CONCLUSIONS

Electron train backgrounds in liquid xenon emission detectors show two distinct components. The amplitude a_1 of the fast component decreases with E_l and appears to be due to thermalized electrons which were not emitted in the primary $S2$ signal. The amplitude a_2 of the slow component increases with E_l and is consistent with the excitation of higher-energy metastable molecular states, whose lifetime is $\gtrsim 1$ ms. De-excitation of these states could be accompanied first by an infrared photon, followed by the usual UV photon. It seems likely that the infrared photon would have enough energy to photoionize electronegative impurities such as O_2^- (which requires about 1/2 eV).

Previous suggestions for mitigation [15] are directed at the τ_1 component, and therefore would not be sufficient for informing the design of discovery-class liquid xenon emission detectors for MeV-scale hidden sector dark matter. The present work suggests two immediate steps towards mitigation of the τ_2 component of electron train backgrounds: (1) a substantial increase in the purity of the liquid xenon target, and (2) an increase in the flow rate of the gaseous xenon above the liquid target. A more speculative possibility includes tuning the gas vapor pressure to limit the maximum energy drifting electrons can attain, thereby prohibiting population of the higher-energy molecular state.

APPENDIX

For a fixed distance d between cathode and anode, and a liquid height $h < d$, the electric field applied in the liquid is given by $E_l = \epsilon_g V / (\epsilon_l d + (\epsilon_g - \epsilon_l)h)$, in which $\epsilon_l = 2$ and $\epsilon_g = 1$ are the long-wavelength limit of the dielectric constants of the liquid and gaseous states. As required by continuity the electric field in the gas is $E_g = \epsilon_l E_l$. Near the cathode grid wires, the electric field increases rapidly in strength. The field profile is analytical [16], but cumbersome to write. Fig. 3 shows the field profile in the case $V = 4$ kV applied to the cathode, directly above one of the cathode wires.

There is some width to the distribution of drift times for alpha particles leaving the cathode, and this particular case is useful for comparison against those events with the shortest (cathode-consistent) drift time. The liquid level was estimated from the profile of E_l , along with the measured electron drift time and known electron drift

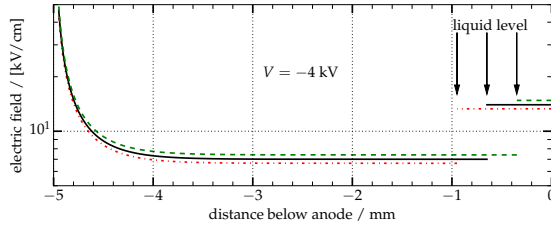


FIG. 3. Calculated electric field as a function of liquid level.

velocity in liquid xenon [17]. Uncertainty in this procedure is estimated to result in a systematic uncertainty of ± 0.4 kV/cm, as indicated in the figures.

ACKNOWLEDGMENTS

This material is based upon work supported by the U.S. Department of Energy, Office of Science, Office of High Energy Physics, under award number DE-AC02-05CH1123.

-
- [1] E. Aprile and T. Doke, *Rev. Mod. Phys.* **82**, 2053 (2010) doi:10.1103/RevModPhys.82.2053 [arXiv:0910.4956 [physics.ins-det]].
 - [2] E.M. Gushchin, A.A. Kruglov and I.M. Obodovskii, *Sov. Phys. JETP* **55** 5 (1982).
 - [3] J. Angle *et al.* [XENON10 Collaboration], *Phys. Rev. Lett.* **107**, 051301 (2011) Erratum: [*Phys. Rev. Lett.* **110**, 249901 (2013)]
 - [4] D. S. Akerib *et al.* [LUX Collaboration], *Phys. Rev. Lett.* **118**, no. 2, 021303 (2017) doi:10.1103/PhysRevLett.118.021303 [arXiv:1608.07648 [astro-ph.CO]].
 - [5] E. Aprile *et al.* [XENON Collaboration], *Phys. Rev. Lett.* **119**, no. 18, 181301 (2017) doi:10.1103/PhysRevLett.119.181301 [arXiv:1705.06655 [astro-ph.CO]].
 - [6] R. Essig, J. Mardon and T. Volansky, *Phys. Rev. D* **85**, 076007 (2012) doi:10.1103/PhysRevD.85.076007 [arXiv:1108.5383 [hep-ph]].
 - [7] R. Essig, T. Volansky and T. T. Yu, *Phys. Rev. D* **96**, no. 4, 043017 (2017) doi:10.1103/PhysRevD.96.043017 [arXiv:1703.00910 [hep-ph]].
 - [8] M. Battaglieri *et al.*, arXiv:1707.04591 [hep-ph].
 - [9] P.E. Figgins, "The Radiochemistry of Polonium," National Academy of Sciences NAS-NS 3037 (1961).
 - [10] B. N. V. Edwards *et al.*, arXiv:1710.11032 [physics.ins-det].
 - [11] J. Jortner, L. Meyer, S.A. Rice and E.G. Wilson, *J. Chem. Phys.* **42** 4250 (1965).
 - [12] S. Kubota, M. Hishida and J. Raun(Gen), *J. Phys. C: Solid State Phys.* **11** 2645 (1978).
 - [13] M.H.R. Hutchinson (1987) Excimer Lasers. In: Mollenauer L.F., White J.C. (eds) *Tunable Lasers. Topics in Applied Physics*, vol 59. Springer, Berlin, Heidelberg
 - [14] W.C. Ermler, Y.S. Lee, K.S. Pitzer and N.W. Winter, *J. Chem. Phys.* **69** 976 (1978).
 - [15] P. Sorensen, arXiv:1702.04805 [physics.ins-det].
 - [16] W. Blum, W. Riegler and L. Rolandi (2008) *Particle Detection with Drift Chambers*, Springer-Verlag, Berlin, Heidelberg
 - [17] E.M. Gushchin, A.A. Kruglov and I.M. Obodovskii, *Sov. Phys. JETP* **55** 4 (1982).